Journal of Pathology
J Pathol 2006; **210**: 363–373
Published online 5 September 2006 in Wiley InterScience
(www.interscience.wiley.com) **DOI:** 10.1002/path.2053

Original Paper

Chemokine receptor expression profiles in nasopharyngeal carcinoma and their association with metastasis and radiotherapy

D-L Ou,[1†] C-L Chen,[2†] S-B Lin,[1] C-H Hsu[3] and L-I Lin[1,4*]

[1] *Department of Clinical Laboratory Sciences and Medical Biotechnology, National Taiwan University, Taiwan*
[2] *Department of Pathology, Taipei Municipal Wanfang Hospital and Taipei Medical University, Taiwan*
[3] *Department of Oncology, National Taiwan University Hospital, Taipei, Taiwan*
[4] *Department of Laboratory Medicine, National Taiwan University Hospital, Taipei, Taiwan*

**Correspondence to:*
Dr L-I Lin, Department of Clinical Laboratory Sciences and Medical Biotechnology College of Medicine, National Taiwan University, 1 Chang-Te St, Taipei, Taiwan.
E-mail: lilin@ha.mc.ntu.edu.tw

[†] *D-LO and C-LC contributed equally to this study.*

Received: 6 January 2006
Revised: 1 July 2006
Accepted: 24 July 2006

Abstract

Nasopharyngeal carcinoma (NPC) is an epithelial cancer that metastasizes predictably to cervical lymph nodes or distant organs. To assess whether the chemokine receptors of NPC cells play important roles in metastasis and are associated with radiotherapy history, the significance of various chemokine receptors (CCR1–10, CXCR1–6, XCR1, and CX3CR1) in NPC cell lines (TW01, TW04, HONE1, BM1, and AS1) and 52 NPC tumour biopsies from 48 patients with NPC was evaluated by mRNA and cytometric analyses, chemotaxis and actin polymerization assays, and immunohistochemical staining. Quantitative real-time reverse transcription-polymerase chain reaction revealed substantial expression of *CCR7, CCR9, CXCR4*, and *CXCR6* mRNA in all the NPC cell lines. Of these, however, only CCR7, CXCR4, and CXCR6 were functional in NPC cells. Negative immunoreactivity for CCR7, CXCR4, and CXCR6 was demonstrated in almost all nasopharyngeal (NP) specimens from patients with primary NPC ($n = 12$) and in those with regional metastatic NPC ($n = 15$). However, expression of two or three of these chemokine receptors was demonstrated in NP specimens from patients with liver metastasis. Strong positivity was demonstrated for all three of these chemokine receptors in almost all of the regional and distant metastasis specimens. Significant differences in the expression of CCR7, CXCR4, and CXCR6 were found between primary tumours and metastases ($p < 0.001$, $p < 0.001$, and $p < 0.002$, respectively). This observation was further confirmed by laser capture microdissection of freshly frozen tumours from primary ($n = 5$) and metastatic ($n = 8$) NPC sites ($p = 0.04$, 0.03, and 0.03 for CCR7, CXCR4, and CXCR6, respectively). Finally, significant differences in CXCR4 expression were demonstrated between *de novo* and post-radiotherapy groups (1/22 vs. 5/8; $p < 0.003$). It appears reasonable to conclude, therefore, that CCR7, CXCR4, and CXCR6 are expressed and active in human NPC metastases, while CXCR4 expression is associated with radiotherapy history.

Keywords: **chemokine receptors; nasopharyngeal carcinoma; metastasis; radiotherapy**

Introduction

Nasopharyngeal carcinoma (NPC) is an epithelial cancer. Unlike cancers of the oral cavity and oropharynx, metastatic nodal disease in NPC frequently appears in the posterior cervical triangle. Bilateral neck nodes are affected by tumour in 53% of patients. Bone, liver, and extra-regional nodes are the most common sites of distant metastases [1].

Metastasis of cancer cells is a complex, highly organized, non-random and organ-selective process. It involves multiple steps, including dissemination of metastasizing cells from the primary tumour, invasion of the surrounding tissue, intravasation and extravasation of the circulatory system, evasion of the immune system, organ-specific targeting, initiation of angiogenesis, and growth advantage at the target organ [2,3]. The target organ for metastasis depends on a variety of factors, such as growth advantage [4,5], the presence of adhesion molecules [6], and chemokine/chemokine receptor (CR) interaction [7]. It is proposed that interplay among these factors might vary across various cancer types.

A complex network of chemokines and their receptors influences the development of primary tumours and metastases [8–10]. Recent studies have

clearly demonstrated the importance of CR expression in metastasis to specific organs (eg lymph nodes, bone marrow, liver and lungs) by breast cancer [11], melanoma [12], and gastric carcinoma cells [13]. CCR6-expressing colon, thyroid, and ovarian carcinoma cells are reportedly associated with hepatic metastasis [14]. It has been demonstrated that CCR9 contributes to the localization of plasma cells to the small intestine [15,16]. CXCR1 and CCR10-expressing melanoma cells may also target endothelial and dermal cells [17,18]. Evidence of an association between specific chemokine(s)/CR(s) and NPC metastasis is limited, except for two recent reports about CXCR4 [19,20]. In this study, therefore, we screened for expression of all known CRs in five NPC cell lines (TW01, TW04, HONE1, BM1, AS1) using quantitative real-time reverse transcription-polymerase chain reaction (qRT-PCR), and then assessed the CR pattern of the NPC cell lines and a variety of tumour tissues samples from 48 patients with NPC using flow cytometry analysis and immunohistochemical (IHC) staining.

Materials and methods

Extraction of RNA from NPC cell lines and RT-PCR

NPC cell lines TW01, TW04, and HONE1 were derived from primary nasopharyngeal tumours from Chinese patients with *de novo* NPC [21–23]. Another two NPC cell lines were derived from metastasized tumour cells in the bone marrow (BM1) and lymph nodes (AS1) of Chinese patients with NPC [24]. These cell lines were a generous gift from Dr Ann-Lii Cheng (Cancer Research Centre, NTUH, Taiwan). Total RNAs were isolated from various cell lines using RNAzol™ B Reagent (Tel-Test, Friendswood, TX, USA) and then reverse transcribed to cDNA using Moloney murine leukaemia virus reverse transcriptase (Epicentre, NJ, USA) with oligo-dT and random hexamer under standard conditions. The primer sequences and PCR conditions for RT-PCR of 18 kinds of CRs were as reported by Nakayama *et al* [25].

Quantitative real-time RT-PCR (qRT-PCR)

Table 1 shows the primers for qRT-PCR of *CXCR4, CXCR6, CCR7*, and *CCR9*, which were designed using Primer Express software (Perkin Elmer Applied Biosystems, Foster City, CA, USA). qRT-PCR was carried out on an ABI Prism 7700 (Perkin Elmer Applied Biosystems) using SYBR green as the detection dye; conditions were 50 °C for 2 min, 95 °C for 10 min, and up to 40 cycles of 95 °C for 15 s (denaturation) and 60 °C for 1 min (annealing/extension). The dissociation curve following the reaction confirmed the specificity of this quantitative assay. The amount of target gene mRNA relative to the internal control gene, *HPRT*, was calculated using the ΔCT method as follows:

$$\text{Relative expression} = 2^{-\Delta CT};\ \text{where } \Delta CT = C_T\ (\text{target gene}) - C_T\ (\text{HPRT}).$$

Flow cytometry analysis

For surface CR detection, 2×10^5 NPC cells were incubated at 2–8 °C for 40 min with non-specific isotype-matched controls and 10–25 μg/ml of each of the following murine monoclonal antibodies: anti-human CXCR4 (clone 44 708.111); anti-human CXCR6 (clone 56 811.111); and, anti-human CCR7 (clone 150 503) or anti-CCR9 (clone 112 509). All of the above antibodies were purchased from R&D Systems, Minneapolis, MN, USA. The mouse primary antibodies were then detected by incubating them at room temperature for 30 min with fluorescein isothiocyanate (FITC)-conjugated goat $(Fab')_2$ anti-mouse IgG (Serotec, UK). The cells were washed twice with phosphate-buffered saline, resuspended, and fixed in 1% (w/v) paraformaldehyde for analysis. Ten thousand cells from each sample were evaluated for fluorescence detection using FACScan (Becton Dickinson, San Jose, CA, USA), and the data were analysed with CellQuest software (Becton Dickinson).

For intracellular CR detection, permeabilized NPC cells were prepared with 0.2% saponin reagent after 4% (w/v) paraformaldehyde fixation, and subjected to the above procedure. These permeabilized cells were maintained in staining buffer containing 0.2% saponin to ensure complete membrane permeabilization throughout.

Chemotaxis assay

Chemotaxis assay was performed in 24-well cell-culture chambers using inserts with 8 μm pores

Table 1. Primer sequences for quantitative real-time RT-PCR analysis and amplicon sizes

	Forward primer	Reverse primer	Amplicon (bp)	Genebank accession number
CCR7	5′-TTCAGTGGCATGCTCCTACTTCT-3′	5′-GCTGAGACAGCCTGGACGAT-3′	71	AY587 876
CCR9	5′-CATTGACGCCTATGCCATGTT-3′	5′-GGTGACCTGGAAGCAGATGTC-3′	73	AJ132 337
CXCR4	5′-TGACCGCTTCTACCCCAATG-3′	5′-AGGATAAGGCCAACCATGATGT-3′	72	AF34 8491
CXCR6	5′-GCCATGACCAGCTTTCACTACA-3′	5′-TTAAGGCAGGCCCTCAGGTA-3′	68	NM_006 564
HPRT	5′-TGACACTGGCAAAACAATGCA-3′	5′-GGTCCTTTTCACCAGCAAGCT-3′	94	M31642

CCR7 = CC chemokine receptor 7; CCR9 = CC chemokine receptor 9; CXCR4 = CXC chemokine receptor 4; CXCR6 = CXC chemokine receptor 6; HPRT = hypoxanthine phosphoribosyl transferase.

(Cambridge, MA, USA, 6.5 mm diameter), the membranes of which were pre-coated with 2.5-μg fibronectin. The upper chamber was seeded with 2×10^4 cells/well, and various chemokines were added to the lower chamber. After incubation for 24 h, the migrated cells attracted by chemokines were attached beneath the membrane. After removing the cells in the upper well with Q-tips, the migrated cells were stained with Liu's stain and quantified by counting five random fields with a light microscope at low power (×100). All experiments were performed in triplicate. The migration index was calculated as follows:

$$\text{Migration index} = \text{migrated cells}_{\text{chemoattract}} / \text{migrated cells}_{\text{serum-free medium}}$$

Actin polymerization assay

Actin polymerization assay was performed according to the standard protocol [26,27]. Briefly, cells were incubated with 150 ng/ml CXCL16 and 100 ng/ml CXCL12 or with 25 μg/ml fibronectin as positive control. At the indicated time points, cells were fixed, permeabilized, and stained in a solution containing 18% paraformaldehyde, 100 μg 1-α-lysophosphatidylcholine (Sigma-Aldrich, St Louis, MO, USA) and FITC-labelled phalloidin (Molecular Probes, Eugene, OR, USA). Actin polymerization was analysed by flow cytometry, with the mean fluorescence ratio of the sample before the addition of chemokine plotted for all time points.

For confocal microscopy analysis, cells were pre-seeded and incubated with 150 ng/ml CXCL16 or assay buffer Dulbecco's modified Eagle's medium for 30 s. Cells were then fixed, permeabilized, and stained with FITC-labelled phalloidin and 100 nM Hoechest (Sigma-Aldrich). Images were visualized with a Leica TCS SP2 confocal spectral microscope (Leica Microsystems GmbH, Heidelberg, Germany).

Patients

From 1993 to 1997, formalin-fixed, paraffin-embedded NPC tissue samples from 48 patients with NPC (Table 2) and freshly frozen tissue samples of NPC tumours from 12 additional NPC patients were collected at the National Taiwan University Hospital (NTUH). This study was approved by the institutional review board of NTUH. Written informed consent was obtained from all patients. Pathologists confirmed the histopathological diagnosis for each specimen. Histopathological classification in these cases was performed according to the revised histological classification for tumours of the upper respiratory tract and ear by the World Health Organization (WHO) in 1991.

Expression study of chemokine receptors in NPC tissues

All the formalin-fixed, paraffin-embedded tissue samples of NPC tumours were sectioned at a thickness of 6 μm and mounted on silane-coated slides (Dako, Carpinteria, CA, USA). After antigen retrieval by heating in a microwave for 5 min with citrate buffer (pH 6.0), these sections were reacted with anti-human CXCR4, anti-human CXCR6, or anti-human CCR7 (R&D Systems) using a standard indirect avidin–biotin–peroxidase method. Breast cancer tumour tissues expressing CRs were used as positive controls. The specificity of immunostaining was also confirmed by use of serial sections with non-immune serum instead of the primary antibody as a negative control. The specimens were evaluated independently without prior knowledge of the clinicopathological information. The results of IHC for each CR were arbitrarily classified according to score, based on the percentage of immunoreactive tumour cells: 0, negative immunostaining; and, 1+, 2+, and 3+ for <10%, 10–50%, and >50% positive immunostaining, respectively.

Laser capture microdissection (LCM)

For quantitative analysis of mRNA of CRs in NPC, freshly frozen primary and metastatic NPC tumour samples were used. The frozen tumour tissues were cut to a thickness of 8 μm. The sections were dehydrated and stained with haematoxylin, and then the tumour cells were microdissected using the Autopix™ system (Arcturus Engineering, Mountain View, CA, USA), according to the manufacturer's instructions. The selected cells were transferred to the LCM transfer film (CapSure TF-100S transfer film carrier, optical-grade transparent plastic, 5 mm diameter; Arcturus Engineering).

The dissected specimens were placed directly into 50 μl of cell lysis buffer consisting of 10 mmol/l Tris-HCl (pH 7.4), 20 mmol/l EDTA, 0.5% sodium dodecyl sulphate, and 20 μl/ml Proteinase K (Wako, Osaka, Japan), and incubated at 45 °C for 30 min. Extraction of total RNA, cDNA synthesis, and real-time PCR were then performed using the above protocols.

Statistical analysis

The statistical significance of the individual findings and their association indices were evaluated using the χ^2 test with Yates' correction. Probability (p) values less than 0.05 were considered significant.

Results

RT-PCR and qRT-PCR analysis reveals that NPC cell lines express different amounts of *CCR7, CCR9, CXCR4*, and *CXCR6* mRNA

A panel of 18 known CRs (CCR1–10, CXCR1–6, XCR1, and CX3CR1) was examined in five NPC

Table 2. Clinicopathological features of the 48 patients with NPC, status at tumour specimen collection, specimen site, and chemokine receptor expression

Patient No	Age	Sex	Histological types*	Staging†	Regional metastasis	Distant metastasis	Treatment status	Tumour specimen	CCR7‡	CXCR4‡	CXCR6‡
1	42	M	IIb	I	N	N	*De novo*	Nasopharynx	0	0	0
2	61	M	IIa	I	N	N	*De novo*	Nasopharynx	0	0	0
3	29	M	IIa	IIB	N	N	*De novo*	Nasopharynx	0	0	0
4	36	M	IIb	IIB	N	N	*De novo*	Nasopharynx	0	0	0
5	35	M	IIb	IIB	N	N	*De novo*	Nasopharynx	0	0	0
6	39	M	IIb	IVA	N	N	*De novo*	Nasopharynx	0	0	0
7	72	M	IIa	—	N	N	*De novo*	Nasopharynx	0	0	0
8	57	F	IIa	IVB	N	N	*De novo*	Nasopharynx	0	0	0
9	43	M	IIa	III	N	N	*De novo*	Nasopharynx	0	0	0
10	47	M	IIb	III	N	N	s/p R/T	Nasopharynx	0	0	0
11	48	M	IIb	II	N	N	s/p C/T	Nasopharynx	0	0	2+
12	47	F	IIb	—	N	N	s/p R/T	Nasopharynx	0	0	0
13	42	F	IIb	IVA	Cervical LN	N	*De novo*	Nasopharynx	0	0	0
14	49	M	IIb	IVA	Cervical LN	N	*De novo*	Nasopharynx	0	0	0
15	34	F	IIb	IVA	Cervical LN	N	*De novo*	Nasopharynx	0	0	0
16	40	M	I	IVA	Cervical LN	N	*De novo*	Nasopharynx	0	0	0
17	58	F	IIb	III	Cervical LN	N	*De novo*	Nasopharynx	0	0	0
18	43	M	IIa	III	Cervical LN	N	*De novo*	Nasopharynx	0	0	1+
19	19	M	IIb	—	Cervical LN	N	*De novo*	Nasopharynx	0	0	0
20	21	F	IIb	III	Cervical LN	N	*De novo*	Nasopharynx	0	0	3+, weak
21	42	M	IIb	IIA	Cervical LN	N	*De novo*	Nasopharynx	0	0	0
22	37	M	IIb	IVA	Cervical LN	N	*De novo*	Nasopharynx	0	0	0
23	39	M	IIb	—	Cervical LN	N	*De novo*	Nasopharynx	0	0	0
24	57	M	IIb	IVB	Cervical LN	N	*De novo*	Nasopharynx	0	0	0
25	63	M	IIa	—	Cervical LN	N	s/p R/T	Nasopharynx	0	0	0

26	67	M	IIa	—	Cervical LN	N	s/p R/T, C/T	Nasopharynx	0	2+	0
27	51	M	IIb	—	Cervical LN	N	s/p R/T	Nasopharynx	0	2+	3+
28	75	M	IIa	II	N	Brain	s/p R/T	Nasopharynx	2+, weak	3+, weak	0
29	68	M	IIb	IVC	N	Liver	*De novo*	Nasopharynx	1+	2+, weak	3+
30	57	M	IIa	—	N	Liver	s/p R/T	Nasopharynx	0	1+, weak	1+, weak
31	43	M	IIb	—	Cervical LN	Brain	s/p R/T	Nasopharynx	3+, weak	1+	3+
32	47	M	IIb	—	Cervical LN	N	s/p R/T, C/T	Neck mass	3+	3+	3+
33	30	M	IIb	III	Cervical LN	N	s/p R/T	Neck mass	3+	3+	3+
34	46	M	IIb	III	Cervical LN	Bone, spleen	*De novo*	Neck mass	3+	3+	3+
35	43	M	IIa	—	Cervical LN	Bone	s/p R/T	Neck mass	3+	3+	3+
36	34	M	IIb	IVC	Cervical LN	Liver, bone	*De novo*	Neck mass	3+	3+	3+
37	59	M	IIb	IVC	Cervical LN	Bone	s/p R/T, C/T	Neck mass	3+	3+	3+
38	51	M	IIb	—	Cervical LN	LN, liver	s/p C/T	Neck mass	3+	3+	3+
39	36	M	IIb	IVC	Cervical LN	Liver, bone	*De novo*	Neck mass	3+	3+	3+
40	70	M	IIb	—	Cervical LN	Bone	*De novo*	Neck mass	3+	3+	3+
41	46	M	IIb	—	Cervical LN	lung	*De novo*	Neck mass	3+	3+	3+
42	61	M	IIb	III	N	Axilla LN	s/p R/T, C/T	Axilla LN	1+	3+	0
43	64	M	IIb	III	N	Inguinal LN, liver, bone	s/p R/T	Inguinal LN	3+	3+	2+
44	51	M	IIb	—	Cervical LN	Bone, liver, abdominal LN	s/p C/T	Abdominal LN	3+	3+	3+
45	39	M	IIb	IVC	N	Axilla LN, bone	s/r R/T, C/T	Axilla LN	3+	3+	3+
46	33	F	IIa	IVC	Cervical LN	Liver, lung	*De novo*	Liver	3+	3+	3+
47	45	M	IIa	II	N	Lung, bone	s/p R/T, C/T	Lung	3+	3+	3+
48	49	M	I	—	N	Liver	s/p R/T	Omentum	0	1+	0

* WHO histological classification of nasopharyngeal carcinoma (1991): I-keratinizing squamous-cell carcinoma; IIa-differentiated non-keratinizing carcinoma; IIb-undifferentiated non-keratinizing carcinoma.

† The 5th edition of the AJCC (American Joint Committee on Cancer) cancer staging for nasopharyngeal carcinoma (1997).

‡ The chemokine receptor expressions were arbitrarily classified by four scores depending on positive immunoreactivity: 0-negative immunostaining; 1+, 2+, 3 + − < 10%, 10–50%, >50% tumour cells with positive immunostaining, respectively; weak-weak positive immunoreactivity.

N-negative; LN-lymph node; *De novo*-without radiotherapy or chemotherapy treatment; s/p R/T-previous radiotherapy treatment; s/p C/T-previous chemotherapy treatment.

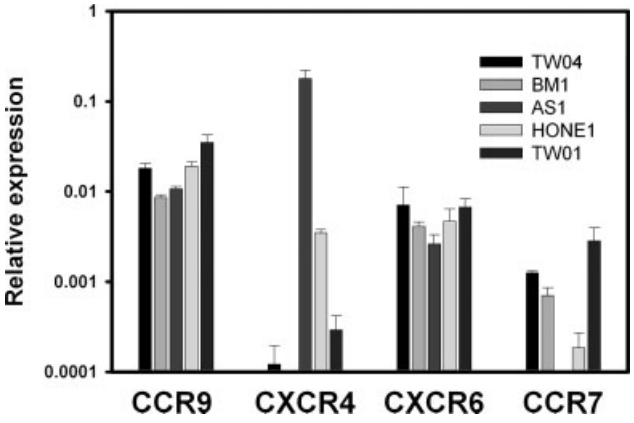

Figure 1. Quantitative real-time RT-PCR analysis of CCR7, CCR9, CXCR4, and CXCR6 expression in NPC cell lines. The cDNA samples were analysed for expression of *CCR7, CCR9, CXCR4, CXCR6* and hypoxanthine phosphoribosyl transferase (*HPRT*) using real-time PCR. The expression of *CCR7, CCR9, CXCR4, CXCR6* was calculated relative to the endogenous control housekeeping gene, *HPRT*, using the ΔCT method (Relative expression $= 2^{-\Delta CT}$; where $\Delta CT = C_{T\ (Target\ gene)} - C_{T\ (HPRT)}$). Values were the mean of two experiments in duplicate ($n = 4$); bars: $\pm$SD

cell lines (TW01, TW04, HONE1, BM1 and AS1) with semi-quantitative RT-PCR, which showed substantial amounts of *CCR7, CCR9, CXCR4*, and *CXCR6* mRNA. Subsequent qRT-PCR revealed that all cell lines demonstrated a similar trend for CR expression of *CCR9 > CXCR6 >CCR7 > CXCR4*, except AS1 cells, which showed abundant *CXCR4* (0.17 : 1 relative to *HPRT*) and little *CCR7* (10^{-4}:1 relative to *HPRT*) expression (Figure 1).

Flow cytometry analysis, migration activity assay, and actin polymerization assay reveal functional CCR7, CXCR4, and CXCR6 in NPC cells

Flow cytometry analysis showed: (i) CXCR4 protein was expressed only on the cell membrane of AS1 cells (in keeping with their high mRNA content); (ii) the CXCR6 protein was expressed on the surface of TW01, TW04, as well as BM1 cells; and (iii) the CCR7 protein was expressed on the surface of TW04 and BM1 cells (Figure 2A). The NPC cells carrying CRs on their membrane also contained the same CRs abundantly in their cytoplasm (data not shown). In contrast, CCR9 was only found in the cytosol but not on the membrane, despite the high mRNA levels of the latter in NPC cells (Figure 2B).

Further Transwell® migration assay verified that CCL21 and CXCL12 could attract migration of NPC cells with surface CCR7 and CXCR4, respectively, just like other carcinoma cells (data not shown). In addition, CXCL16 attracted migration of TW01 and TW04 cells (both CXCR6 positive) in a dose-dependent manner, but the same results were not obtained with BM1 cells even if they expressed substantial CXCR6 on the membrane (Figure 3A): this may be explained by the substantially higher spontaneous migration of BM1 cells, relative to TW01, TW04, and HONE 1 cells (136.3 ± 5.3/LPF, 18.8 ± 1.3/LPF, 28.8 ± 3.9/LPF, 33.1 ± 0.9/LPF, respectively).

Further actin polymerization assay by flow cytometry and confocal microscopy revealed that 150 ng/ml CXCL16 induced a transient 1.7-fold increase in intracellular F-actin content in TW01 cells within 15 s (Figure 3B), and showed distinct pseudopodia formation and intense F-actin staining near the periphery of the TW01 cells treated with CXCL16 (Figure 3C), suggesting that the morphological changes triggered by the interaction between CXCR6 and CXCL16 are prerequisites for TW01 cell mobility. Similar phenomena were observed when TW04 was exposed to CXCL16 (data not shown).

Significant differences in CXCR4, CXCR6, and CCR7 expression between primary and metastatic tissues; only CXCR4 expression is associated with radiotherapy history

IHC staining of CCR7, CXCR4, and CXCR6 showed that these CRs were detected in both cytoplasm and membrane of metastatic tumour tissues, but not in primary NPC tumours (Figure 4). Table 2 summarizes the treatment status for the patients with NPC at the time of tumour specimen collection, the associated site, and CR expression. We found that nasopharyngeal (NP) specimens from patients with primary NPC ($n = 12$) all showed negative immunoreactivity for CCR7, CXCR4 and CXCR6, except for one case (patient 11), who had previously received chemotherapy treatment. Negative immunoreactivity was also demonstrated for all NP specimens from patients with regional metastatic NPC ($n = 15$), except for those from four individuals (patients 18, 20 26, 27). Heterogeneous expression of CXCR4, CCR7, and CXCR6 was demonstrated for NP specimens from liver metastasis cases (patients 29 and 30). These results were similar to those for the above-described primary NPC cell lines, TW01, TW04, and HONE1. However, specimens from regional and distant metastases (neck mass, axilla and inguinal lymph node, lung, and liver) were strongly positive for all three CRs (patients 32–48), except for those from two subjects (patients 42 and 48). Intriguingly, NP specimens from brain-invasion cases (patients 28 and 31) were also CXCR4 and CCR7 positive to different extents. Three of these individuals also had sequential evaluations (patients 9, 40, and 41), which revealed associations between CR expression and the existence of metastasis as well as its type (data not shown). Overall statistical analysis of the expression of these three CRs in NPC cases with metastasis demonstrated significant differences between tumours from primary and metastatic sites (Table 3). Furthermore, significant differences were demonstrated only for CXCR4 when nasopharyngeal specimens from patients with or without radiotherapy history were compared (5/8 vs. 1/22;

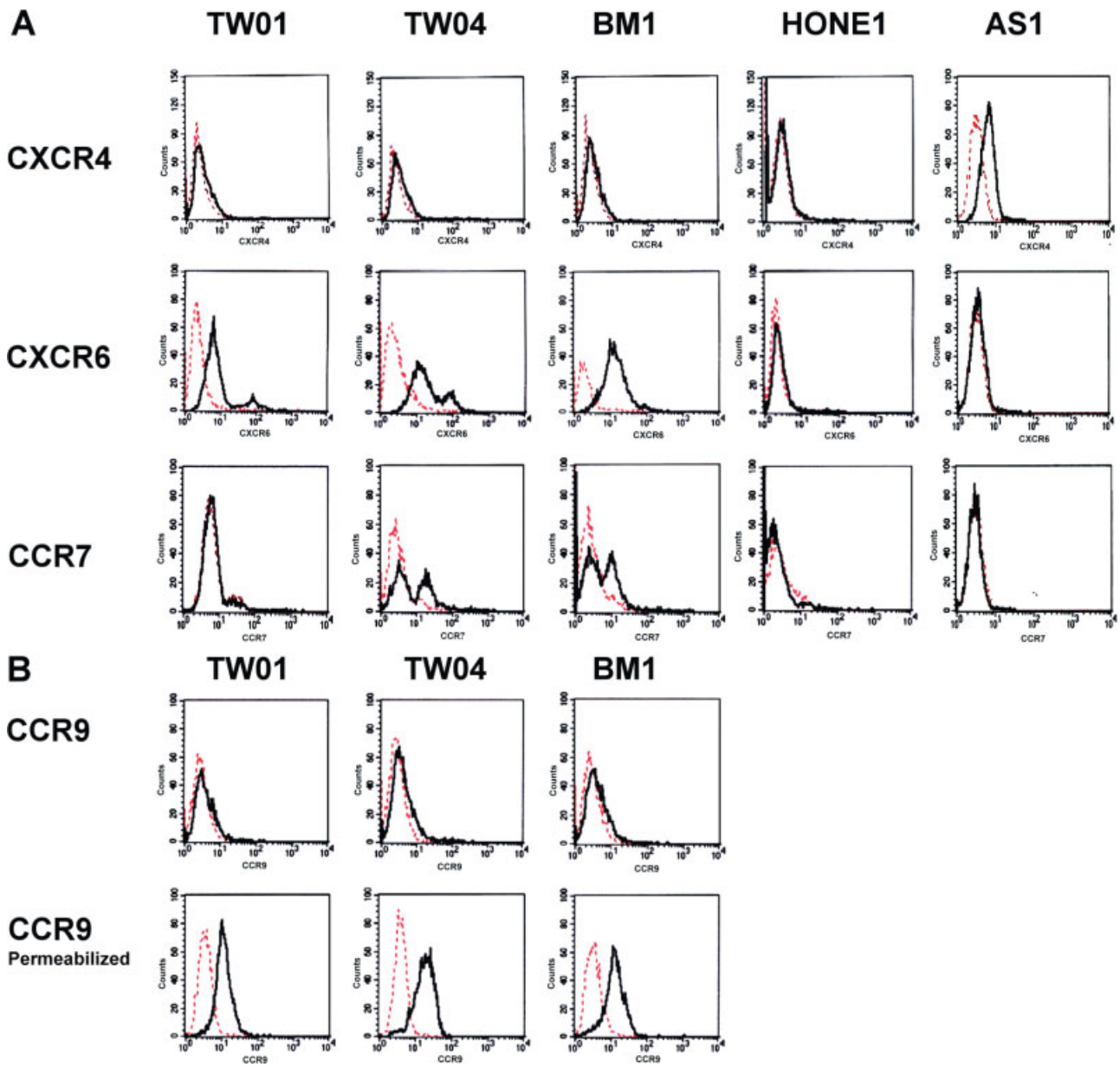

Figure 2. Flow cytometry analysis of surface or intracellular expression of CCR7, CCR9, CXCR4, and CXCR6 by NPC cell lines. (A) Flow cytometry analysis at the surface of CCR7, CXCR4, and CXCR6 by NPC cell lines. Cells were incubated with various monoclonal antibodies directed against CCR7, CXCR4, and CXCR6 (bold lines) with an isotype-matched control (dashed lines). (B) Surface and intracellular CR analysis by flow cytometry. Both permeabilized and non-permeabilized cells were analysed for surface and intracellular CCR9 expression with monoclonal antibodies directed against CCR9 (bold lines) and with an isotype-matched control (dashed lines). The x-axis represents fluorescence intensity and the y-axis represents cell count. Representative results from three independent experiments are shown

$p < 0.003$), while no relationship was demonstrated between CCR7 and CXCR6 and radiotherapy history (Table 3).

To assess the expression of CR RNA in NPC tumour tissues further, we evaluated 13 freshly frozen NPC tumour samples from 12 additional patients with NPC. Of these, paired NP and metastasis specimens were studied from one patient, and only NP or metastasis specimen from the other patients. LCM coupled with qRT-PCR was used to compare the relative mRNA amount in NP specimens ($n = 5$) and metastases ($n = 8$) (as mean $\pm$ SD), respectively, as follows: *CCR7* to *HPRT* (internal control gene), 0.029 ± 0.051 and 0.437 ± 0.367 ($p = 0.04$); *CXCR4* to *HPRT*, 0.209 ± 0.281, and 1.389 ± 0.824 ($p = 0.03$); *CXCR6* to *HPRT*, 0.005 ± 0.008 and 0.191 ± 0.091 ($p = 0.03$). The differences between the NP specimens and metastases were statistically significant for all comparisons, with these results consistent with the IHC findings. As to the only paired specimen, all three CR mRNAs were present in substantial amounts in the metastasis and in only low amounts in the NP specimen.

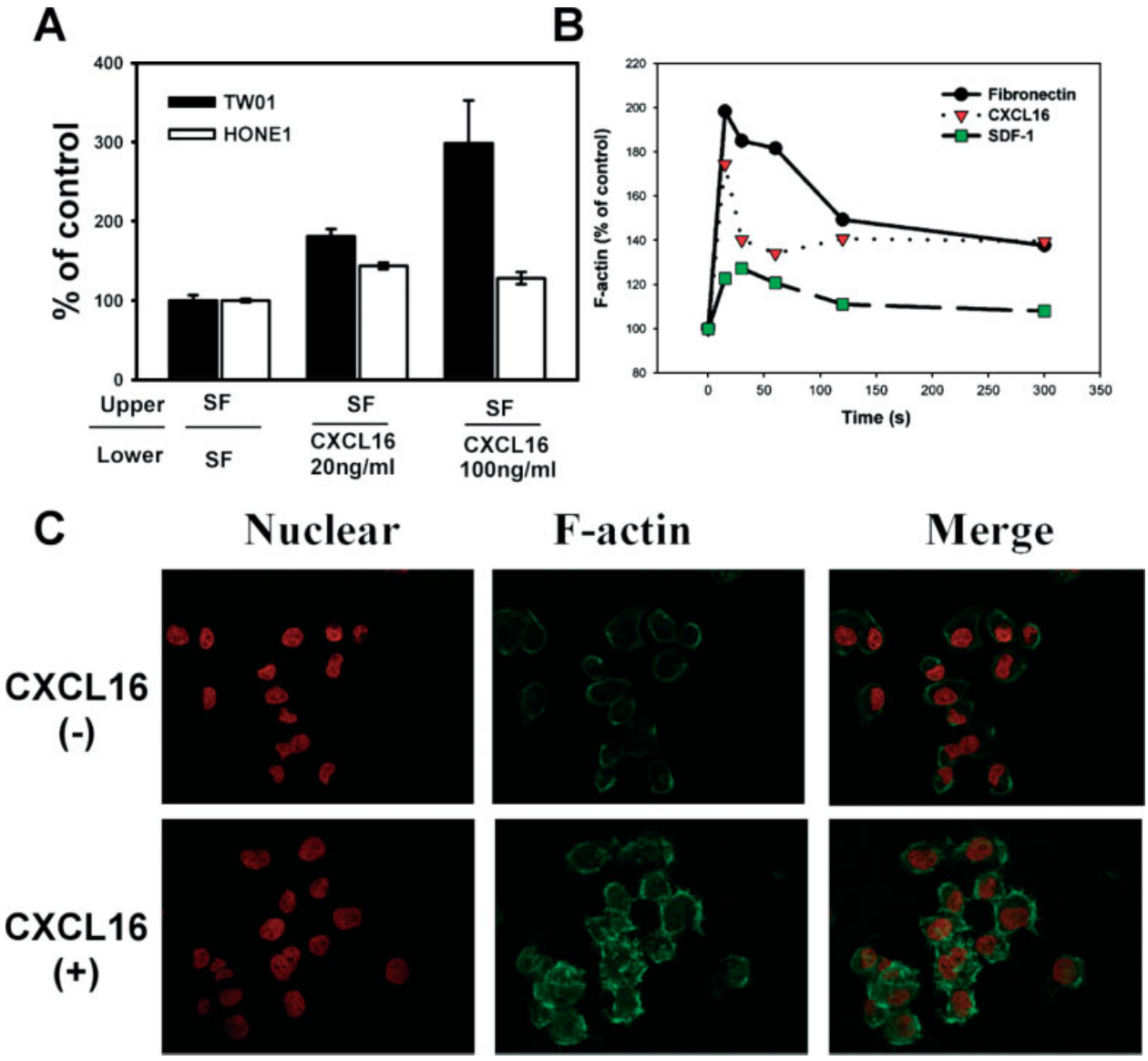

Figure 3. Functional assays for CXCR6 on NPC cells. (A) Chemotaxis of NPC cells across transwell membranes precoated with fibronectin. CXCL16 was added to the lower chamber at the indicated concentrations. Chemotaxis across the membrane was assessed after 24 h. The cells on the lower side of the membrane were stained and counted by microscopy from five low-power fields. (B) Actin polymerization assay of F-actin polymerization in TW01 cells. TW01 cells were incubated with 150 ng/ml CXCL16, 100 ng/ml CXCL12 (also named SDF-1), or 25 μg/ml fibronectin as a positive control. At the indicated time points, actin polymerization was analysed by flow cytometry, and the mean fluorescence ratio of those samples before adding chemokine plotted for all time points. (C) Confocal microscopy analysis of F-actin polymerization in TW01 cells. TW01 cells were stimulated with or without 150 ng/ml CXCL16 for 30 s. Images were acquired using a Leica TCS SP2 confocal spectral microscope (Leica Microsystems)

Discussion

During the preparation of this paper, two reports investigating the relationship between CXCR4 and NPC were considered. Wang *et al* found that high CXCR4 expression was associated with poor overall survival [19], while Hu *et al* showed that expression of functional CXCR4 is associated with the metastatic potential of human NPC cells [20]. In this study, a comprehensive *in vitro* and *in vivo* survey for CR expression revealed that, in addition to CXCR4, CCR7 and CXCR6 were significant in NPC metastasis. Further, only CXCR4 expression was associated with radiotherapy history.

Our *in vitro* data show that NPC cells can express CCR7, CXCR4, and CXCR6 both in the cytoplasm and on cell membranes. It has been shown that: CCL21, a ligand for CCR7, is highly expressed in lymph nodes [11]; CXCL12, a ligand for CXCR4, is moderately expressed in lymph node, lung, liver, and bone marrow [11]; and CXCL16, a ligand for CXCR6, is highly expressed in lung and liver [28,29] and moderately expressed in lymph node [30]. Therefore, the expression of CCR7, CXCR4, or CXCR6 in NPC tumour cells may be responsible for the potential of NPC to metastasize to lymph node, bone, liver, and lung [1]. However CCR9 proteins remain in the cytoplasm and are not expressed on the cell membrane,

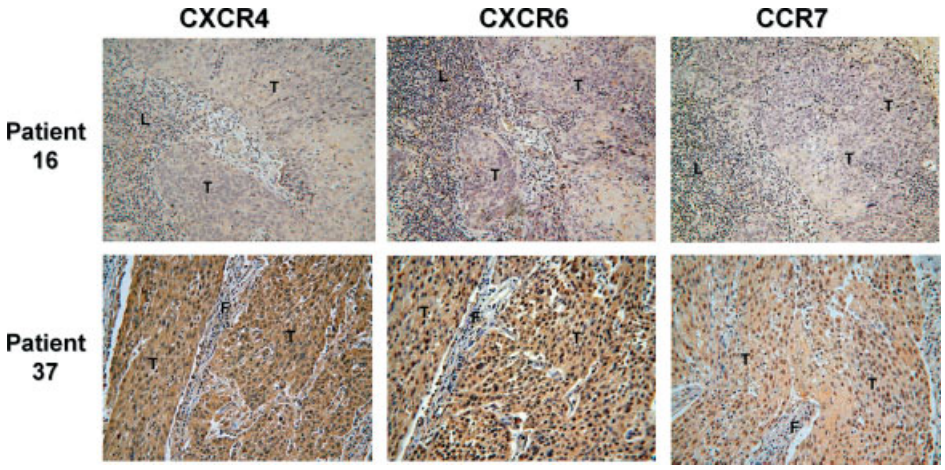

Figure 4. Immunohistochemical staining of CCR7, CXCR6, and CXCR4 in NPC tumour tissues. Representative CR expressions from primary nasopharygyneal sites of *de novo* NPC (patient 16) and from a neck mass of metastatic NPC (patient 37). Images were acquired using a light microscope. T = tumour region; L = lymphocytes; F = fibroblasts

Table 3. Comparison of chemokine receptor expression in primary, metastatic, and post-radiotherapy tumours

	CCR7†		CXCR4†		CXCR6†	
Tumour type	**Positive**	**Negative**	**Positive**	**Negative**	**Positive**	**Negative**
NP tumour (n = 31)						
From NPC patients with metastasis (n = 19)	3	16	6	13	6	13
From NPC patients without metastasis (n = 12)	0	12	0	12	1	11
p Value	0.410		0.089		0.286	
NPC patients with metastasis (n = 36)						
NP tumour (n = 19)	3	16	6	13	6	13
Metastases (n = 17)	16	1	17	0	15	2
p Value	<0.001*		<0.001*		<0.002*	
NP tumour (n = 30)						
From NPC patients without radiotherapy (n = 22)	1	21	1	21	3	19
From NPC patients after radiotherapy (n = 8)	2	6	5	3	3	5
p Value	0.335		<0.003*		0.353	

* Significant difference between groups stated.
† Chemokine receptor expressions evaluated as stated in Table 1; negative-0; positive-1+–3+.

which may explain why NPC cells do not usually metastasize to the intestine, which contains abundant CCL25, a ligand of CCR9 [15,31]. Nude mouse transplantation experiments with TW01 cell lines [21] demonstrated that many small metastatic granules are disseminated in the lung parenchyma, and a few in the liver. These results are consistent with our finding of only CXCR6 expression on the surface membrane of TW01 cells. Further, CXCR6/CXCL16 signalling has recently been associated with liver-specific homing [32–35] and lung-specific homing [36,37]. Here, we also show that the CRs expressed on the NPC cell membrane are functional, as shown by the biological consequences, including chemotaxis and actin polymerization, induced by their cognate ligands. Accordingly, the circulating NPC cells with functional CR might arrive and proliferate at distant metastatic sites where the respective ligands are expressed. Recently, Scala's group also reported a similar mechanism, with CXCR4 being expressed and active in human melanoma metastases [38].

Our *in vivo* data reveal, using IHC analysis of tumour biopsy specimens from NPC patients with metastasis, that there is heterogeneous expression of CXCR4, CCR7, and CXCR6 in the primary tumour specimens of patients with regional or distant metastasis, and abundant expression of these CRs in the metastatic NPC of analogues with regional or distant metastasis. CR expression was detected in both cytoplasm and membrane in these metastases. Similar features were reported in tumour biopsies from breast cancer, colorectal cancer, melanoma, and squamous cell carcinoma [38–41]. Two possibilities are suggested for the differential expression of CR between primary and metastatic NPC. One is that cancer cells with CR expression in primary NP tumours may be selected for distant metastasis, and the other is that environmental factors may up-regulate CR expression in metastasizing cells [42–44]. The latter possibility has been supported by several studies using *in vitro* cell systems, which revealed cytokine-mediated induction of CXCR4 expression [42,45].

Another interesting finding from our IHC analysis of NPC tissues is that CXCR4 expression was significantly associated with positive radiotherapy history. Recently, several studies have proposed that cancer cells undergo a hypoxia–reoxygenation process after radiotherapy, which then leads to nuclear accumulation of hypoxia-induced factor-1α (HIF-1α) [46,47], and subsequently to the regulation of HIF-1α-responsive genes such as *CXCR4* and *VEGF* [48,49]. Staller *et al* also provided convincing evidence that *CXCR4* is an HIF-1α-regulated gene, whose expression can be negatively regulated by the von Hippel–Lindau protein [50]. Therefore, the HIF-1α–CXCR4 pathway may regulate trafficking in and out of hypoxic tissue microenvironments and trigger a homing mechanism that enables the migrating cells to target specific organs [51]. These findings are consistent with our finding of high CXCR4 expression by NPC tumour cells in post-radiotherapy patients. As CXCR4 is a prominent HIV-1 receptor, several inhibitors for it have been recently generated as potential therapies to block HIV-1 infection, and consequently, may theoretically block direct interactions between CXCR4 and CXCL12. Hence, our finding may be useful in the future development of novel strategies for targeting hypoxic NPC tumours.

Acknowledgements

We are grateful to Dr Ann-Lii Cheng (Cancer Research Centre, National Taiwan University Hospital, Taiwan) for his valuable suggestions. Supported in part by grant NSC93-2314-B002-265 from National Science Council, Taiwan

References

1. Fandi A, Altun M, Azli N, Armand JP, Cvitkovic E. Nasopharyngeal cancer: epidemiology, staging, and treatment. *Semin Oncol* 1994;**21:**382–397.
2. Engers R, Gabbert HE. Mechanisms of tumor metastasis: cell biological aspects and clinical implications. *J Cancer Res Clin Oncol* 2000;**126:**682–692.
3. Stetler-Stevenson WG, Kleiner DE Jr. Molecular biology of cancer: invasion and metastases. In *Cancer: principles and practice of oncology* (6th edn), DeVita VT Jr, Hellman S, Rosenberg SA (eds), Lippincott Williams & Willkins: Philadelphia, 2001; 123–136.
4. Liotta LA. An attractive force in metastasis. *Nature* 2001;**410:**24–25.
5. Liotta LA, Saidel MG, Kleinerman J. The significance of hematogenous tumor cell clumps in the metastatic process. *Cancer Res* 1976;**36:**889–894.
6. Nicolson GL. Molecular mechanisms of cancer metastasis: tumor and host properties and the role of oncogenes and suppressor genes. *Curr Opin Oncol* 1991;**3:**75–92.
7. Chambers AF, Groom AC, MacDonald IC. Dissemination and growth of cancer cells in metastatic site. *Nature Rev Cancer* 2000;**2:**563–572.
8. Taub DD. Chemokine–leukocyte interactions. The voodoo that they do so well. *Cytokine Growth Factor Rev* 1996;**7:**355–376.
9. Zlotnik A, Yoshie O. Chemokines: a new classification system and their role in immunity. *Immunity* 2000;**12:**121–127.
10. Rollins BJ. Chemokines. *Blood* 1997;**90:**909–928.
11. Muller A, Homey B, Soto H, Ge N, Catron D, Buchanan ME, *et al*. Involvement of chemokine receptors in breast cancer metastasis. *Nature* 2001;**410:**50–56.
12. Murakami T, Maki W, Cardones AR, Fang H, Tun Kyi A, Nestle FO, *et al*. Expression of CXC chemokine receptor-4 enhances the pulmonary metastatic potential of murine B16 melanoma cells. *Cancer Res* 2002;**62:**7328–7334.
13. Mashino K, Sadanaga N, Yamaguchi H, Tanaka F, Ohta M, Shibuta K, *et al*. Expression of chemokine receptor CCR7 is associated with lymph node metastasis of gastric carcinoma. *Cancer Res* 2002;**62:**2937–2941.
14. Dellacasagrande J, Schreurs OJ, Hofgaard PO, Omholt H, Steinsvoll S, Schenck K, *et al*. Liver metastasis of cancer facilitated by chemokine receptor CCR6. *Scand J Immunol* 2003;**57:**534–544.
15. Pabst O, Ohl L, Wendland M, Wurbel MA, Kremmer E, Malissen B, *et al*. Chemokine receptor CCR9 contributes to the localization of plasma cells to the small intestine. *J Exp Med* 2004;**199:**411–416.
16. Letsch A, Keilholz U, Schadendorf D, Assfalg G, Asemissen AM, Thiel E, *et al*. Functional CCR9 expression is associated with small intestinal metastasis. *J Invest Dermatol* 2004;**122:**685–690.
17. Ramjeesingh R, Leung R, Siu KH. Interleukin-8 secreted by endothelial cells induces chemotaxis of melanoma cells through the chemokine receptor CXCR1. *FASEB J* 2003;**17:**1292–1294.
18. Murakami T, Cardones AR, Finkelstein SE, Restifo NP, Klaunberg BA, Nestle FO, *et al*. Immune evasion by murine melanoma mediated through CC chemokine receptor-10. *J Exp Med* 2003;**198:**1337–1347.
19. Wang N, Wu Q-L, Fang Y, Mai H-Q, Zeng M-S, Shen G-P, *et al*. Expression of chemokine receptor CXCR4 in nasopharyngeal carcinoma: pattern of expression and correlation with clinical outcome. *J Transl Med* 2005;**3:**26.
20. Hu J, Deng X, Bian X, Li G, Tong Y, Li Y, *et al*. The expression of functional chemokine receptor CXCR4 is associated with the metastatic potential of human nasopharyngeal carcinoma. *Clin Cancer Res* 2005;**11:**4658–4665.
21. Lin CT, Wong CI, Chan WY, Tzung KW, Ho JK, Hsu MM, *et al*. Establishment and characterization of two nasopharyngeal carcinoma cell lines. *Lab Invest* 1990;**62:**713–724.
22. Lin CT, Chan WY, Chen W, Huang HM, Wu HC, Hsu MM, *et al*. Characterization of seven newly established nasopharyngeal carcinoma cell lines. *Lab Invest* 1993;**68:**716–727.
23. Yao KT, Zhang HY, Zhu HC, Wang FX, Li GY, Wen DS, *et al*. Establishment and characterization of two epithelial tumor cell lines (HNE-1 and HONE-1) latently infected with Epstein–Barr virus and derived from nasopharyngeal carcinomas. *Int J Cancer* 1990;**45:**83–89.
24. Liao SK, Perng YP, Shen YC, Chung PJ, Chang YS, Wang CH. Chromosomal abnormalities of a new nasopharyngeal carcinoma cell line (NPC-BM1) derived from a bone marrow metastasis lesion. *Cancer Genet Cytogenet* 1998;**103:**52–58.
25. Nakayama T, Fujisawa R, Izawa D, Hieshima K, Takada K, Yoshie O. Human B cells immortalized with Epstein–Barr virus upregulate CCR6 and CCR10 and downregulate CXCR4 and CXCR5. *J Virol* 2002;**76:**3072–3077.
26. Carulli G, Sbrana S, Minnucci S, Azzara A, Angiolini C, Gullaci AR, *et al*. Actin polymerization in neutrophils from patients affected by myelodysplastic syndromes — a flow cytometric study. *Leuk Res* 1997;**21:**513–518.
27. Merry C, Puri P, Reen DJ. Phosphorylation and the actin cytoskeleton in defective newborn neutrophil chemotaxis. *Pediatr Res* 1998;**44:**259–264.
28. Shimaoka T, Kume N, Minami M, Hayashida K, Kataoka H, Kita T, *et al*. Molecular cloning of a novel scavenger receptor for oxidized low density lipoprotein, SR-PSOX, on macrophages. *J Biol Chem* 2000;**275:**40663–40666.
29. Wilbanks A, Zondlo SC, Murphy K, Mak S, Soler D, Langdon P, *et al*. Expression cloning of the STRL33/BONZO/TYMSTR ligand reveals elements of CC, CXC, and CX3C chemokines. *J Immunol* 2001;**166:**5145–5154.
30. Nakayama T, Hieshima K, Izaqa D, Tatsumi Y, Kanamaru A, Yoshie O. Cutting edge: profile of chemokine receptor expression on human plasma cells accounts for their efficient recruitment to target tissues. *J Immunol* 2003;**170:**1136–1140.

31. Kunkel EJ, Campbell JJ, Haraldsen G, Pan J, Boisvert J, Roberts AI, *et al*. Lymphocyte CC chemokine receptor 9 and epithelial thymus-expressed chemokine (TECK) expression distinguish the small intestinal immune compartment: epithelial expression of tissue-specific chemokines as an organizing principle in regional immunity. *J Exp Med* 2000;**192:**761–768.
32. Kim CH, Kunkel EJ, Boisvert J, Johnston B, Campbell JJ, Genovese MC, *et al*. Bonzo/CXCR6 expression defines type 1-polarized T-cell subsets with extralymphoid tissue homing potential. *J Clin Invest* 2001;**107:**595–601.
33. Geissmann F, Cameron TO, Sidobre S, Manlongat N, Kronenberg M, Briskin MJ, *et al*. Intravascular immune surveillance by CXCR6+ NKT cells patrolling liver sinusoids. *PLoS Biol* 2005;**3:**e113.
34. Sato T, Thorlacius H, Johnston B, Staton TL, Xiang W, Littman DR, *et al*. Role for CXCR6 in recruitment of activated CD8+ lymphocytes to inflamed liver. *J Immunol* 2005;**174:**277–283.
35. Heydtmann M, Lalor PF, Eksteen JA, Hubscher SG, Briskin M, Adams DH. CXC chemokine ligand 16 promotes integrin-mediated adhesion of liver-infiltrating lymphocytes to cholangiocytes and hepatocytes within the inflamed human liver. *J Immunol* 2005;**174:**1055–1062.
36. Agostini C, Cabrelle A, Calabrese F, Bortoli M, Scquizzato E, Carraro S, *et al*. Role for CXCR6 and its ligand CXCL16 in the pathogenesis of T-cell alveolitis in sarcoidosis. *Am J Respir Crit Care Med* 2005;**172:**1290–1298.
37. Morgan AJ, Guillen C, Symon FA, Huynh TT, Berry MA, Entwisle JJ, *et al*. Expression of CXCR6 and its ligand CXCL16 in the lung in health and disease. *Clin Exp Allergy* 2005;**35:**1572–1580.
38. Scala S, Giuliano P, Ascierto PA, Ierano C, Franco R, Napolitano M, *et al*. Human melanoma metastases express functional CXCR4. *Clin Cancer Res* 2006;**12:**2427–2433.
39. Kim J, Takeuchi H, Lam ST, Turner RR, Wang HJ, Kuo C, *et al*. Chemokine receptor CXCR4 expression in colorectal cancer patients increases the risk for recurrence and for poor survival. *J Clin Oncol* 2005;**23:**2744–2753.
40. Ding Y, Shimada Y, Maeda M, Kawabe A, Kaganoi J, Komoto I, *et al*. Association of CC chemokine receptor 7 with lymph node metastasis of esophageal squamous cell carcinoma. *Clin Cancer Res* 2003;**9:**3406–3412.
41. Wang J, Xi L, Hunt JL, Gooding W, Whiteside TL, Chen Z, *et al*. Expression pattern of chemokine receptor 6 (CCR6) and CCR7 in squamous cell carcinoma of the head and neck identifies a novel metastatic phenotype. *Cancer Res* 2004;**64:**1861–1866.
42. Jourdan P, Vendrell J-P, Huguet M-F, Segondy M, Bousquet J, Pene J, *et al*. Cytokines and cell surface molecules independently induce CXCR4 expression on CD4 + CCR7+ human memory T cells. *J Immunol* 2000;**165:**716–724.
43. Bachelder RE, Wendt MA, Mercurio AM. Vascular endothelial growth factor promotes breast carcinoma invasion in an autocrine manner by regulating the chemokine receptor CXCR4. *Cancer Res* 2002;**62:**7203–7206.
44. Nanki T, Shimaoka T, Hayashida K, Taniguchi K, Yonehara S, Miyasaka N. Pathogenic role of the CXCL16-CXCR6 pathway in rheumatoid arthritis. *Arthritis Rheum* 2005;**52:**3004–3014.
45. Nagase H, Miyamasu M, Yamaguchi M, Fujisawa T, Ohta K, Yamamoto K, *et al*. Expression of CXCR4 in eosinophils: functional analyses and cytokine-mediated regulation. *J Immunol* 2000;**164:**5935–5943.
46. Moeller BJ, Cao Y, Li CY, Dewhirst MW. Radiation activates HIF-1 to regulate vascular radiosensitivity in tumors: role of reoxygenation, free radicals, and stress granules. *Cancer Cell* 2004;**5:**429–441.
47. Semenza GL. Intratumoral hypoxia, radiation resistance, and HIF-1. *Cancer Cell* 2004;**5:**405–406.
48. Bernards R. Cancer: cues for migration. *Nature* 2003;**425:**247–248.
49. Le QT, Denko NC, Giaccia AJ. Hypoxic gene expression and metastasis. *Cancer Metastasis Rev* 2004;**23:**293–310.
50. Staller P, Sulitkova J, Lisztwan J, Moch H, Oakeley EJ, Krek W. Chemokine receptor CXCR4 downregulated by von Hippel-Lindau tumour suppressor pVHL. *Nature* 2003;**425:**307–311.
51. Schioppa T, Uranchimeg B, Saccani A, Biswas SK, Doni A, Rapisarda A, *et al*. Regulation of the chemokine receptor CXCR4 by hypoxia. *J Exp Med* 2003;**198:**1391–1402.